Research Square

Preprints are preliminary reports that have not undergone peer review.
They should not be considered conclusive, used to inform clinical practice,
or referenced by the media as validated information.

Colour ranks but does not measure mild thermal modification: optical, gravimetric, hygroscopic and structural responses of Avodire (Turraeanthus africanus) wood treated in dry air

Jerry Oppong Adutwum

joadutwum@csir-forig.org.gh

CSIR–Forestry Research Institute of Ghana (CSIR- FORIG)

Akosua Anowuo Asamoah

CSIR–Forestry Research Institute of Ghana (CSIR- FORIG)

Georgina Konadu Opoku

CSIR–Forestry Research Institute of Ghana (CSIR- FORIG)

James Kofi Korang

CSIR–Forestry Research Institute of Ghana (CSIR- FORIG)

Emmanuel Ebanyenle

CSIR–Forestry Research Institute of Ghana (CSIR- FORIG)

Francis Wilson Owusu

CSIR–Forestry Research Institute of Ghana (CSIR- FORIG)

Research Article

Keywords:

Posted Date: November 9th, 2026

DOI: https://doi.org/10.21203/rs.3.rs-11648538/v1

License: This work is licensed under a Creative Commons Attribution 4.0 International License.
Read Full License

Additional Declarations: No competing interests reported.

Colour ranks but does not measure mild thermal modification: optical, gravimetric, hygroscopic and structural responses of Avodire (*Turraeanthus africanus*) wood treated in dry air

Jerry Oppong Adutwum[1,*], Akosua Anowuo Asamoah[1], Georgina Konadu Opoku[1], James Kofi Korang[1], Emmanuel Ebanyenle[1], Francis Wilson Owusu[1]

[1]Wood Industry and Utilisation Division, CSIR–Forestry Research Institute of Ghana (CSIR-FORIG), Kumasi, Ghana

*Corresponding author: joadutwum@csir-forig.org.gh

Abstract

Thermal-modification severity is often inferred from wood colour, assuming that colour change tracks mass loss, hygroscopicity and dimensional change, an assumption rarely tested in mild regimes or for tropical hardwoods. We tested whether the optical, gravimetric, hygroscopic and structural responses of Avodire share a common onset and form during dry-air treatment. Specimens from one lot of kiln-dried boards were treated at 160, 180, 200 and 220 °C for 3 h ($n = 10$ per group) and compared with a 105 °C drying control. CIELAB colour, anhydrous weight loss (AWL), dimensions, density and 14-day moisture uptake were measured on the same specimens; inference is restricted to this lot. Reddening, total colour difference and 14-day moisture content differed from the control from 160 °C; AWL did too, but only by water that 105 °C drying retains, and dry-matter loss was first detected at 180 °C. The domains separated partly by onset and mainly by magnitude and form. Drying-corrected ΔE^*_{ab} rose from 3.4 to 31.1 while AWL reached only 2.85 %. Colour change was proportional to AWL, but the 180 °C group produced less colour per unit AWL (6.8, against 10.2–10.9). Lightness loss began at 180 °C, whereas Δb^* was non-monotonic. Treatment lowered moisture-uptake capacity and lengthened its timescale, while one Weibull shape ($\beta = 0.72$) described all curves. A radial-shrinkage and densification anomaly occurred at 180 °C only. Colour can rank treatment severity within a calibrated process, but it is not a quantitative surrogate for mass loss, hygroscopic capacity or structural state.

Keywords: Anhydrous weight loss; CIELAB colour; Moisture sorption; Thermal modification; *Turraeanthus africanus*

1 Introduction

1.1 One driver, several responses

Thermal modification heats wood to 160–240 °C to improve its dimensional stability, durability and appearance, and is an established commercial route to modified timber (Sandberg et al. 2021; Esteves and Pereira 2008; Hill 2006). The atmosphere matters as well: treatment under oxidizing conditions in air (dry thermal treatment) increases carbonyl groups and decreases hydroxyl groups, whereas treatment in steam or water (hygrothermal, or wet, treatment) accelerates the acid-catalysed hydrolysis of the hemicelluloses (Inagaki et al. 2018). The present study uses dry thermal treatment in air. Treatment temperature and time are the external drivers. They set off a connected set of cell-wall reactions: deacetylation and depolymerisation of the hemicelluloses, transformation and loss of extractives, formation of chromophores, and condensation of lignin (Candelier et al. 2016; Esteves and Pereira 2008; Tjeerdsma and Militz 2005). These reactions are observed through different measurements. Colour reports the optical consequence of chromophore formation; anhydrous weight loss (AWL) reports the net departure of volatile substance; moisture content after conditioning reports accessible sorption sites; dimensions and density report the geometry of the cell wall and the stresses it carried during treatment. Nothing requires these proxies to share one threshold or one temperature dependence. A common driver can nonetheless produce strong correlations among them even when the underlying responses are neither proportional nor mechanistically equivalent, and this distinction between pooled correlation and genuine coupling is the subject of this study.

1.2 Colour as a practical but potentially biased severity indicator

Total colour difference (ΔE^*_{ab}) is attractive as a process indicator because it is rapid, inexpensive and non-destructive, can be measured in line, and responds at low treatment severity (Bytner et al. 2022; Candelier et al. 2016; Brischke et al. 2007). Treated wood loses lightness (L^*), gains redness (a^*) and changes yellowness (b^*) non-monotonically (Bytner et al. 2022; González-Peña and Hale 2009). Using colour as a severity proxy implicitly assumes either proportionality between colour and material degradation or a stable calibration between colour and the property of interest. The assumption can fail in three ways: the responses may start at different temperatures; they may have different temperature sensitivities, so that the ratio between them

drifts; or one of them may follow a non-monotonic or pathway-specific trajectory. Each failure has a different consequence for process control, so they need to be separated empirically rather than inferred from one pooled correlation.

1.3 Unresolved issues in the mild-treatment regime

Severe treatments generate both conspicuous darkening and appreciable mass loss, and in that regime colour and mass loss move together almost by necessity. The mild regime, with short holds and mass loss of a few per cent, is more diagnostic, because early optical reactions may proceed before gravimetric or hygroscopic changes become measurable; it is also the regime used for high-value appearance products. Two further issues are rarely addressed. First, aggregate ΔE^*_{ab} can conceal different trajectories in ΔL^*, Δa^* and Δb^*, which arise from different chemical events (Matsuo et al. 2011). Second, moisture measurements are usually reduced to one terminal moisture content, which cannot show whether treatment changes the capacity, the timescale or the shape of moisture uptake.

1.4 Study system and questions

Avodire (*Turraeanthus africanus* (Welw.) Pellegr.; Meliaceae) is a West and Central African hardwood of moderate density valued for its pale, creamy-yellow figure in decorative veneer and joinery (Owusu 2008). The mean lightness (L^* = 80.32) classifies it as a high-lightness species (Nishino et al. 1998). Its light natural colour makes it a sensitive substrate for detecting small optical changes. Published modification research on the species is limited to a thermo-chemical treatment, polyglycerol methacrylate impregnation followed by heating at 150–240 °C under nitrogen, assessed for durability and termite resistance (Quartey et al. 2025); the colour, dry-matter and moisture-uptake responses to heat treatment in air have not been reported. Because the specimens came from one supply lot, the study is exploratory and its comparisons are within-lot.

We asked whether the optical, gravimetric, hygroscopic and structural responses of Avodire evolve along one common severity axis or show distinct thresholds, sensitivities and forms. Four expectations follow from the alternative to a single axis: (E1) optical change begins at a lower temperature than detectable AWL; (E2) the CIELAB components follow distinct temperature trajectories, so that ΔE^*_{ab} is a composite response; (E3) treatment changes moisture-uptake

capacity and timescale more than the normalised shape of the uptake curve; and (E4) the structural response is not necessarily monotonic in temperature. These expectations were formulated after an earlier analysis of the same data and are therefore tested here in an exploratory, not a confirmatory, sense. The corresponding objectives were to map the treatment effect in every domain against a common control (Sect. 3.1); to decompose the optical response (Sect. 3.2); to test how colour relates to AWL within and across temperatures (Sect. 3.3); to separate capacity, timescale and shape of moisture uptake (Sects. 3.4 and 3.5); and to characterise the structural response (Sect. 3.6).

2 Materials and methods

2.1 Material provenance and inferential scope

Kiln-dried, defect-free boards of Avodire were supplied by a sawmill in the Western North Region of Ghana. The boards were flat-sawn. Fifty clear specimens free of knots, reaction wood and irregular grain were cut to nominal dimensions of 99.3 ± 0.2 mm (longitudinal) × 50.1 ± 0.2 mm (width, tangential direction) × 15.3 ± 0.2 mm (thickness, radial direction), with a mean as-received mass of 41.3 ± 1.8 g. Dimensions were measured to 0.01 mm with a digital caliper (Mitutoyo CD-6" CS) and mass to 0.01 g. Specimens were randomly assigned to five groups of ten: a control and four treatment temperatures. As-received density and pre-treatment lightness did not differ among groups (Kruskal–Wallis $p = 0.29$ and 0.67).

The specimens are subsamples of one supply lot whose tree of origin was not recorded. They are therefore not independent biological replicates, and statistical inference in this paper is restricted to this lot and this treatment run; the p-values do not describe variation among trees or among Avodire populations.

2.2 Thermal treatment and control

Specimens were placed in a laboratory oven (GENLAB OV95CF, England) at 100 ºC and held there for 1 h. The oven was then heated at 20 ºC/h to 160, 180, 200 or 220 ºC, and the target temperature was held for 3 h. The ramp therefore added 3, 4, 5 and 6 h between 100 ºC and the target, so total thermal exposure increased with the target temperature beyond the common 3h holding time. After the hold, the oven was cooled gradually to 100 ºC; the specimens were then removed and cooled in a desiccator before post-treatment mass and dimensions were kept in the laboratory for a few days before the second oven-drying (Sect. 2.4). The atmosphere was laboratory air; no inert gas was used, so the optical response may include oxidative reactions (Inagaki et al. 2018) that nitrogen, steam or oxygen-limited industrial processes would attenuate.

The control specimens were oven-dried at 105 °C for 24 h and were measured in the same sequence as the treated specimens. The control is therefore a 105 °C drying control, not untreated wood, and every treatment effect reported here is the change beyond that produced by drying at 105 °C.

2.3 Colour measurement

Surface colour was measured with a Nix Mini 3 contact colour sensor (Nix Sensor Ltd, Hamilton, Canada; 15 mm aperture) under illuminant D65 and the 2 ° standard observer, on the planed tangential face. Ten readings per face were averaged before and after treatment. The same marked locations were re-measured after treatment. The sensor is a low-cost instrument rather than a laboratory spectrophotometer, and its repeatability was not characterised separately.

For each specimen we computed ΔL^*, Δa^* and Δb^* as post- minus pre-treatment values, chroma C^*_{ab} and hue angle h_{ab}, the metric hue difference ΔH^*_{ab}, and the total colour difference

$$\Delta E^*_{ab} = (\Delta L^{*2} + \Delta a^{*2} + \Delta b^{*2})^{1/2}. \qquad (1)$$

The treatment effect on colour was estimated as a contrast with the control group (Sect. 2.9). For description, a drying-corrected colour difference was also computed,

$$\Delta E^*_{ab,\mathrm{dc}} = \Delta E^*_{ab} - \overline{\Delta E^*_{ab}}_{\mathrm{control}}, \qquad (2)$$

which removes the mean colour change caused by drying at 105 °C but does not remove the specimen-level uncertainty of the control measurement.

2.4 Anhydrous weight loss

The pre-treatment oven-dry mass of each specimen was estimated from its conditioned mass and the mean initial moisture content of the controls,

$$\widehat{m}_{0,\mathrm{dry}} = \frac{m_{\mathrm{conditioned}}}{1 + \mathrm{MC}_0/100}, \qquad \mathrm{AWL} = 100\,\frac{\widehat{m}_{0,\mathrm{dry}} - m_{\mathrm{post}}}{\widehat{m}_{0,\mathrm{dry}}}, \qquad (3)$$

where m_{post} is the mass weighed immediately after treatment and $\mathrm{MC}_0 = 10.91 \pm 0.33$ % (mean $\pm$ SD) was obtained from the same weighing step on the controls, that is, from their mass after 24 h at 105 °C. Numerator and baseline therefore come from one weighing step, and the control AWL is zero by construction. A batch-average MC_0 shifts every treated group by the same amount and does not alter the contrasts with the control; it does add specimen-level scatter, because the controls' own moisture content ranged from 10.8 to 11.9 % (this scatter is visible as the control AWL SD of 0.30 percentage points). The balance resolution (0.01 g on about 40 g)

contributes less than 0.03 percentage points per weighing. Before the uptake test, all specimens were oven-dried again at 105 °C for 24 h; for treated specimens this second oven-dry mass was 0.16–0.51 % higher than the post-treatment mass, so it was used only as the reference for moisture content during uptake and not for AWL. Because the post-treatment mass was weighed after drying at the treatment temperature, it refers to a drier state than the 105 °C state on which $\widehat{m}_{0,\mathrm{dry}}$ is based, and AWL from Eq. 3 therefore also contains water that the treatment removed and 105 °C drying retains. As a lower bound on dry-matter loss, AWL was recomputed from the second oven-dry mass with MC_0 from the controls' second drying (11.11 %), so that both masses refer to the 105 °C state (Table S3). Eq. 3 remains the primary measure.

2.5 Dimensions, density and estimated porosity

Shrinkage along each axis was computed from as-received to post-treatment dimensions, volume retention as post-treatment over as-received volume, and swelling as the volume change from post-treatment to the end of the 14-day uptake. Oven-dry density was the post-treatment mass divided by the post-treatment volume, and porosity was estimated as

$$\phi_{\mathrm{est}} = 1 - \rho_{\mathrm{oven\text{-}dry}}/\rho_{\mathrm{cell\text{-}wall}}, \qquad (4)$$

with an assumed cell-wall substance density of 1.50 g cm^{-3}. ϕ_{est} is an indirect estimate that follows from density, not a measured pore volume.

2.6 Moisture uptake

After the second oven-drying, specimens were exposed to ambient laboratory air and weighed after 24, 48, 144, 192, 216, 288, 312 and 336 h. Relative humidity was not controlled. Because mass constancy was not demonstrated and RH was not controlled, the final value is reported as the 14-day terminal moisture content, MC_{336}, rather than an equilibrium moisture content. Moisture-exclusion efficiency was $\mathrm{MEE} = 100\,(\overline{\mathrm{MC}_{336}}_{\mathrm{control}} - \mathrm{MC}_{336})/\overline{\mathrm{MC}_{336}}_{\mathrm{control}}$.

2.7 Sorption models and master curve

Each uptake curve was fitted with

$$M(t) = M_{\infty}\left[1 - \exp\left(-(t/\tau)^{\beta}\right)\right], \qquad (5)$$

where M_∞ is the fitted uptake capacity, τ the characteristic timescale and β an empirical curve-shape parameter. β is not interpreted here as a distribution of physical relaxation times, because no independent derivation supports that reading. Four treatments of β were compared on the same 400 observations by the corrected Akaike information criterion (AICc), each with specimen-specific M_∞ and τ: $\beta = 1$ (first-order uptake), one β shared by all specimens, one β per group, and one β per specimen. The shared and group estimates were obtained by profiling the residual sum of squares over a β grid of step 0.005, with 95 % intervals from 4000 specimen bootstrap resamples. As a separate check on model form, a short-time Fickian law ($F = kt^{1/2}$), a power law ($F = kt^n$) and a two-parameter Weibull were ranked per curve by AIC on uptake normalised by its 336 h value.

For the master curve, time was rescaled as $t^* = t/\tau_i$ and uptake as $F = M(t)/M_{\infty,i}$, using each specimen's parameters under the shared β. The quality of collapse was summarised by the root-mean-square residual about $F = 1 - \exp[-(t^*)^\beta]$, overall and by group. One control specimen (TA-C-6) reads 7.1 % at 192 h, below its 144 h value of 9.1 %; all sorption analyses were repeated without it.

2.8 Colour amplification and the colour–AWL relationship

The colour–AWL relationship was examined at three levels: the pooled regression of ΔE^*_{ab} on AWL across all 50 specimens; group centroids with 95 % intervals; and a temperature-conditioned model for the 40 treated specimens,

$$\mathrm{AWL}_i = \alpha + \beta_1 \, \Delta E^*_{ab,i} + \gamma_{T(i)} + \varepsilon_i, \qquad (6)$$

with a separate intercept γ_T for each temperature and HC3 standard errors; a version with linear temperature in place of γ_T was also fitted. β_1 asks whether colour carries information about AWL beyond their shared dependence on temperature. The colour-amplification factor, $\mathrm{CAF}_T = \overline{\Delta E^*_{ab,\mathrm{dc}_T}}/\overline{\mathrm{AWL}_T}$, was computed with a 95 % interval from 4000 bootstrap resamples of treated and control specimens. CAF was interpreted only where AWL was clearly above zero.

2.9 Statistical analysis

Each treated group was compared with the control for each response. Effects are reported as differences in group means with Welch 95 % confidence intervals and as Hedges g with approximate 95 % intervals. Because several groups departed from normality (minimum Shapiro–Wilk $p = 0.001$ for AWL), p-values were obtained from two-sided permutation tests (9999 permutations, seed 42). They were Holm-adjusted within four predefined response families: optical (ΔL^*, Δa^*, Δb^*, ΔE^*_{ab}), gravimetric (AWL), hygroscopic (MC_{336}, M_∞, τ) and structural (radial and tangential shrinkage, volume retention, oven-dry density, estimated porosity, swelling). The onset of a response is the lowest temperature at which the adjusted $p < 0.05$. Onsets depend on test power as well as on the wood, so they are read together with the effect sizes. All analyses are exploratory. Apparent Arrhenius slopes are reported only in the Supplementary material, because one hold time cannot provide rate constants or activation energies. Analyses used Python 3.12 (SciPy 1.17, statsmodels 0.14).

3 Results

3.1 The response domains share an onset but not a form

Every domain except the structural one contained a response that departed from the drying control at the lowest treatment temperature (Fig. 1, Table 2). At 160 °C, reddening, yellowing, total colour difference, AWL from the post-treatment mass and MC_{336} already differed from the control, whereas lightness, uptake capacity M_∞, uptake timescale τ and every structural measure first differed at 180 °C. Expectation E1 was supported for dry-matter loss but not for AWL as measured: AWL from the post-treatment mass differed from the control at 160 °C, depending on the test, but by no more than the water removed beyond the 105 °C state; on the 105 °C basis the 160 °C contrast was -0.03 percentage points ($p = 0.84$) and dry-matter loss was first detected, marginally, at 180 °C ($p_{\mathrm{Holm}} = 0.046$; Sect. 3.3, Table S3). The domains differed instead in how they changed. Lightness loss was small at 160 and 180 °C and large above; yellowing peaked and reversed; colour change per unit AWL was lower at 180 °C than at 200 and 220 °C; τ peaked at 200 °C; and the structural measures departed from the control at 180 °C alone.

3.2 Optical change contains several trajectories

Post-treatment lightness fell from 78.2 in the control to 76.7, 74.5, 62.4 and 46.5 at 160–220 °C (Fig. 2, Table S1). Relative to the control, ΔL^* did not differ at 160 °C (-0.4; 95 % CI -2.5 to 1.7) and differed modestly at 180 °C (-3.7; -6.3 to -1.1; $p_{\mathrm{Holm}} = 0.014$) before falling steeply to -16.4 and -31.0 at 200 and 220 °C. Redness rose monotonically and differed at every temperature (Δa^* contrast 1.4, 2.9, 5.8 and 8.1; $p_{\mathrm{Holm}} \leq 0.002$). Yellowness rose through 200 °C (contrast 3.4, 5.3 and 5.6) and fell back at 220 °C (1.5; -0.1 to 3.1) and no longer differed from the control. Hue angle fell from 82.8 ° in the control to 65.8 ° at 220 °C, a rotation from yellow toward orange-red.

The total colour difference combined these trajectories. ΔE^*_{ab} was 3.6 in the control and 7.1, 10.7, 21.8 and 34.8 after treatment, so $\Delta E^*_{ab,\mathrm{dc}}$ was 3.4, 7.1, 18.1 and 31.1, and all four contrasts differed from the control. At 160 °C, ΔE^*_{ab} was carried mainly by Δb^*; at 220 °C, by ΔL^*. ΔE^*_{ab} therefore combines an early monotonic component (redness), a component with a higher threshold (lightness) and a non-monotonic component (yellowness), consistent with E2. A single

number cannot be read as one reaction coordinate when its dominant component changes with temperature.

3.3 Colour ranks treatment severity but does not measure mass loss

AWL was 0.31 ± 0.35, 1.04 ± 0.32, 1.78 ± 0.54 and 2.85 ± 0.42 % at 160–220 °C (Fig. 3a). The 160 °C contrast was small and its interval almost reached zero (0.31; 0.003 to 0.62; $p_{\mathrm{Holm}} = 0.045$). A rank-based comparison across all five groups (Kruskal–Wallis with Holm-adjusted Dunn tests) did not separate 160 °C from the control ($p = 0.34$), so the onset of AWL at 160 °C depends on the test. From 180 °C the difference was unambiguous. On the 105 °C basis the values were -0.03, 0.35, 1.32 and 2.45 % (Table S3); the difference between the two bases, water rather than dry matter, was 0.34 to 0.68 percentage points and largest at 180 °C. Dry-matter loss at 160 °C therefore cannot be distinguished from zero, and at 180 °C it lies between 0.35 and 1.04 %.

Across all 50 specimens ΔE^*_{ab} was strongly related to AWL ($r = 0.95$; $\Delta E^*_{ab} = 3.6 + 10.1\,\mathrm{AWL}$, slope 95 % CI 9.1 to 11.1; Fig. 3b). Its intercept (95 % CI 1.9 to 5.2) matches the mean ΔE^*_{ab} of the control (3.6), that is, the colour change produced by drying at 105 °C. Among the treated specimens, the drying-corrected colour difference was on average proportional to AWL ($\Delta E^*_{ab,\mathrm{dc}}$ intercept -0.4, 95 % CI -2.8 to 2.0; slope 10.3, 8.8 to 11.8), so this experiment provides no evidence of treatment-induced colour change at zero AWL. The group centroids did not all lie on that line. The colour-amplification factor was 6.8 (95 % CI 5.8 to 7.9) at 180 °C, 10.2 (9.1 to 11.5) at 200 °C and 10.9 (10.0 to 11.9) at 220 °C (Fig. 3c), so a given colour difference corresponded to more mass loss at 180 °C, the temperature of the structural anomaly (Sect. 3.6), than at the higher temperatures. At 160 °C the interval was 4.7 to 29.7, and CAF is not interpreted there. Within each temperature, specimens with more colour change also lost more mass: holding temperature constant, AWL rose by 0.076 percentage points per ΔE^*_{ab} unit (95 % CI 0.040 to 0.113; 0.058, 0.031 to 0.086, with linear temperature; Fig. 3d). Colour therefore carries information about AWL beyond their common dependence on temperature, but with a calibration that shifts between temperatures.

3.4 Moisture capacity and timescale respond with different patterns

MC_{336} fell from 10.76 ± 0.23 % in the control to 10.39, 10.10, 8.97 and 7.43 % (Fig. 4). The reduction was small but already detectable at 160 °C (-0.37; -0.58 to -0.17; $p_{\mathrm{Holm}} = 0.006$) and became large at 200 and 220 °C (-1.8 and -3.3 percentage points); MEE reached 3.5, 6.2, 16.6 and 30.9 %. The fitted capacity M_∞ followed MC_{336} closely (11.06 in the control to 7.81 % at 220 °C) but first differed from the control at 180 °C. The characteristic time did not follow the same pattern. τ was 52.9 h in the control and did not change at 160 °C, then lengthened to 67.7 and 80.3 h at 180 and 200 °C before shortening to 73.2 h at 220 °C. Across specimens MC_{336} was correlated with ΔE^*_{ab} ($r = -0.97$) and with AWL ($r = -0.92$); these pooled correlations follow from the shared temperature series and do not by themselves show proportional coupling.

3.5 Normalised uptake curves share an approximately invariant shape

In the per-curve comparison of short-time laws, the two-parameter Weibull was ranked first for 47 of 50 curves (Fickian law 2, power law 1). Median half-uptake times were 30 h in the control and 35–48 h in the treated groups, every t_{90} fell within the 14-day record, and no free fit reached a parameter bound (Table S4). In the joint fit (Table S2), a single shared β was strongly preferred over first-order uptake (ΔAICc = 474) and over one β per specimen (ΔAICc = 164). The shared estimate was $\beta = 0.72$ (95 % CI 0.70 to 0.73). Allowing one β per group gave ΔAICc = 8.6 against the shared model with all curves, and 0.1 without TA-C-6, so the data neither require nor exclude a group effect on shape. The group estimates declined slightly with temperature, from 0.745 at 160 °C to 0.685 at 220 °C.

Rescaling each curve by its own M_∞ and τ placed all specimens on one master curve (Fig. 5) with a residual RMSE of 0.018 in units of F (0.013 to 0.014 for each treated group; 0.014 overall without TA-C-6). The residuals had the same systematic pattern in every group (Fig. 5d), so the Weibull form misfits all groups in the same way rather than misfitting the treated groups differently. Within this experiment, treatment therefore changed the capacity and timescale of uptake much more than its normalised shape, consistent with E3, with the qualification that a decline in β of about 0.06 across the temperature range cannot be excluded.

3.6 The structural response is non-monotonic

The 180 °C group differed from the control on every structural measure, while the other groups hardly differed (Fig. 6, Table 2). Its radial shrinkage was 8.2 ± 0.3 % against 2.4 ± 0.5 % in the control (contrast 5.8; 5.4 to 6.2), and its tangential shrinkage was 3.8 ± 1.3 % (contrast 1.3; 0.4 to 2.3; not significant after adjustment). The radial-to-tangential shrinkage ratio was 2.2 at 180 °C and 0.8 to 1.2 in the other groups. Longitudinal shrinkage also rose (1.13 against 0.18 to 0.25 %). Volume retention fell to 87.3 % (contrast -7.7), oven-dry density rose to 0.574 g cm^{-3} (contrast 0.068; 0.041 to 0.096), estimated porosity fell to 0.617, and swelling during uptake reached 14.1 % against 5.0 % in the control. At 220 °C swelling was slightly smaller than in the control (-1.2; $p_{\mathrm{Holm}} = 0.005$), and volume retention was 0.8 points lower, at the edge of significance ($p_{\mathrm{Holm}} = 0.050$). The 180 °C pattern had no counterpart in the colour, AWL or moisture-capacity series, none of which showed a discontinuity at that temperature (E4).

4 Discussion

4.1 One treatment does not produce one material-state variable

The responses to a single thermal driver differed in form, sensitivity and magnitude even where their statistical onsets coincided (Table 3). Redness rose early and monotonically; lightness loss had a higher threshold and accelerated; yellowness accumulated and then reversed; mass loss stayed small; moisture capacity fell mainly at 200 and 220 °C; the uptake timescale peaked at 200 °C; the normalised uptake shape barely moved; and the structure changed at 180 °C alone. Strong pooled correlations among these readouts (ΔE^*_{ab}–AWL $r = 0.95$, ΔE^*_{ab}–MC_{336} $r = -0.97$) are what a common driver produces. They do not by themselves show proportional or causal coupling. Colour and AWL were close to proportional on average once the drying effect was removed, but the 180 °C group departed from that proportion, and the structural anomaly had no optical counterpart.

The onset result needs qualification. In an earlier analysis of the same data, a rank-based test across all groups placed the AWL and ΔE^*_{ab} onsets at 200 and 180 °C; direct permutation contrasts with the control place both at 160 °C. An onset is the first temperature at which a test crosses its threshold, so it depends on power and on the AWL definition as well as on the wood. For this reason we base the comparison between domains on effect sizes and trajectories rather than on onset temperatures.

4.2 Why optical change can exceed net mass loss

At 220 °C, a drying-corrected colour difference of 31 units accompanied an AWL of only 2.85 %. A small amount of chemical transformation can change visible-light absorption strongly without a comparable loss of volatile mass. Possible contributors include oxidation or transformation of extractives, formation of conjugated carbonyl groups, reactions of lignin side chains, and dehydration products retained in the cell wall (Esteves and Pereira 2008; Tjeerdsma and Militz 2005) surface oxidation may be favoured in dry air. None of these was measured, so they remain candidate explanations. Measurement sensitivity also contributes. Colour is measured at the surface, AWL is a bulk quantity, and AWL rests on an estimated rather than a measured pre-treatment oven-dry mass. The 0.31 % AWL at 160 °C is a case in point: on the 105 °C basis it falls to -0.03 % (Table S3), so it is water that drying at 160 °C removes and 105 °C drying

retains rather than degraded substance. We therefore do not interpret AWL below about 0.5 % as evidence of material degradation.

4.3 Why ΔE^*_{ab} should not be treated as a single kinetic variable

Because ΔL^*, Δa^* and Δb^* followed different trajectories, any activation-like parameter fitted to ΔE^*_{ab} depends on the temperature range: the dominant component shifts from yellowing and reddening at 160 °C to darkening at 220 °C. Apparent temperature sensitivities computed from one hold time (Supplementary material) illustrate the point, with lightness loss the most sensitive and reddening the least, but they are descriptors, not activation energies. A working model consistent with the data has an early pathway expressed mainly as reddening, a pathway with a higher threshold expressed as darkening, and accumulation of yellow chromophores followed by their transformation or masking above 200 °C. Matsuo et al. (2011) likewise resolved different temperature dependences for the CIELAB coordinates. Chemical analysis would be needed to test this model, and comparisons of single ΔE^*_{ab} kinetics between species are likely to mislead unless the component trajectories and the atmosphere are matched.

4.4 Moisture uptake changes in scale more than in form

The moisture results separate into three effects. Lower terminal and fitted capacity suggests fewer or less accessible sorption sites, which is consistent with partial removal of hygroscopic hemicellulose (Repellin and Guyonnet 2005; Metsä-Kortelainen et al. 2006), although cell-wall composition was not measured. The longer characteristic time means that treated wood approached its terminal state more slowly; the shortening of τ from 200 to 220 °C has no explanation in the present data. The approximately invariant normalised shape indicates that treatment mainly rescaled the uptake response rather than producing an obviously new kinetic regime.

In complex-systems terms, the collapse is approximate self-similarity under time rescaling,

$$F_i(t) \approx \mathcal{F}(t/\tau_i), \qquad (7)$$

with one function $\mathcal{F}$ for all specimens and treatment entering through τ_i and $M_{\infty,i}$. This is an empirical statement about curve shape, not a statement that the diffusion mechanism is unchanged; testing that would require controlled geometry, dense early-time sampling and

independent cell-wall or pore measurements. The result does make a falsifiable prediction: further hold times or atmospheres should shift capacity and timescale while preserving $\mathcal{F}$ only if the same coarse-grained uptake dynamics remain at work.

4.5 The 180 °C anomaly as a competing-mechanism problem

The anomaly was coherent across radial shrinkage, volume retention, density, estimated porosity and swelling, and it had no counterpart in the optical, gravimetric or hygroscopic-capacity responses. The structural event is therefore at least partly decoupled from the chemical indicators. Two explanations compete. In the mechanistic explanation, the cell wall softens within a narrow temperature interval enough to deform under drying stresses, before higher-temperature reactions stiffen and set it. The combination of excess anisotropic shrinkage, densification and large recoverable swelling is consistent with a collapse-like event (Navi and Sandberg 2009; Blakemore and Langrish 2008; Kauman 1964), although its cellular basis cannot be identified from macroscopic measurements. In the design-based explanation, the 180 °C group coincided with different board material, anatomical variation, growth stresses or a different oven position or heating rate. Group allocation was random, but board identity, specimen position and ring orientation were not recorded, so this explanation cannot be excluded. A gravimetric observation points the same way: the second oven-dry mass exceeded the post-treatment mass most at 180 °C (0.51 against 0.16–0.29 % in the other treated groups; Table S3), so after re-humidification the 180 °C specimens held the most water at the 105 °C state. The near-equal radial and tangential shrinkage of the control (2.4 and 2.4 %) suggests that growth rings were not parallel to the specimen faces. Decisive tests are repeat treatments with several boards and trees and mapped specimen positions, light microscopy or micro-CT, X-ray density profiles, dynamic mechanical analysis across 160–220 °C, and core-temperature and humidity logging during treatment.

4.6 Implications for colour-based process monitoring

Within a defined and calibrated process, colour can rank treatment severity: it rose monotonically with temperature, separated all four temperatures from the control, and within a temperature it carried information about AWL. It is also the natural control variable for appearance products. Its use as a quantitative surrogate is limited by three results. First, drying at 105 °C alone produced ΔE^*_{ab} of 3.6, so any reading needs a drying baseline from the same

measurement sequence. Second, the colour-to-AWL ratio was not the same at every temperature. Third, colour did not register the structural response at all. Any colour–AWL or colour–MC_{336} calibration is therefore conditional on species, supply lot, surface preparation, atmosphere, sensor, hold time and initial moisture content. The separate CIELAB coordinates are more informative than ΔE^*_{ab}: Δa^* responds early, while ΔL^* reports the higher-severity regime.

A practical alternative is to describe treatment state by several variables rather than one, for example

$$\boldsymbol{S} = [\Delta L^*,\ \Delta a^*,\ \mathrm{AWL},\ M_\infty,\ \tau]. \qquad (8)$$

For appearance-driven production, monitoring ΔL^* and Δa^* may be sufficient. Hygroscopic performance needs validation against moisture-capacity measurements, and structural quality cannot be inferred from colour. The present data do not support claims that colour predicts mechanical strength or durability, that 200–220 °C treatment suits outdoor service, or that one CAF value applies across production batches.

4.7 Limitations

The limitations define the boundaries of inference. First, all specimens came from one supply lot with unrecorded board and tree identity, so there is no biological replication. Second, one hold time and one atmosphere (dry air) were used. Third, pre-treatment oven-dry masses were estimated from a batch moisture content, and the 105 °C reference retains water that higher treatment temperatures remove, which places dry-matter loss between the two bases of Table S3. Fourth, colour was measured with a low-cost sensor on one face, without separate repeatability data. Fifth, moisture uptake was followed in uncontrolled ambient air for 14 days, with the first weighing at 24 h; early-time behaviour was therefore sparsely sampled. Sixth, neither chemical composition, anatomy, mechanical properties nor biological durability was measured. Seventh, board position, ring orientation and oven position were not recorded and may confound the 180 °C anomaly.

4.8 Falsifiable predictions and next experiments

The results suggest five tests. (i) Longer holds at 160–180 °C should increase darkening and AWL without changing the normalised uptake shape. (ii) Treatment under nitrogen should

reduce the early optical response if oxidation contributes substantially. (iii) Species or boards with different extractive chemistry should show different colour amplification at low severity. (iv) If the 180 °C feature is a true collapse window, it should recur in independent boards and appear in anatomical images or density profiles. (v) If the master-curve scaling holds generally, it should survive independent boards, additional hold times and denser early-time sampling.

5 Conclusions

1. Optical change preceded dry-matter loss, and the domains differed in form. Reddening, total colour difference and 14-day moisture content differed from the 105 °C control from 160 °C; AWL from the post-treatment mass did too, but only by the water that treatment removes beyond the 105 °C state, so dry-matter loss was first detected at 180 °C, together with lightness, uptake capacity, uptake timescale and structure.

2. Colour was composite. Reddening rose monotonically, lightness loss had a higher threshold, and yellowness rose and reversed, so ΔE^*_{ab} should not be interpreted as a single mechanistic coordinate.

3. Colour ranked but did not measure mass loss. Once the drying effect was removed, ΔE^*_{ab} was on average proportional to AWL and also tracked AWL within each temperature, yet the colour change per unit AWL was 6.8 at 180 °C against 10.2 and 10.9 at 200 and 220 °C.

4. Moisture uptake separated into capacity, timescale and shape. Treatment lowered capacity and lengthened the characteristic time, while one Weibull shape ($\beta = 0.72$) described all curves, with at most a small decline at higher temperature.

5. Structure followed a separate, non-monotonic trajectory. The 180 °C group showed excess radial shrinkage with densification, which requires replication with independent boards and anatomical verification.

Colour can support calibrated appearance control and relative severity ranking, but it cannot independently certify the gravimetric, hygroscopic, structural, mechanical or durability state of thermally modified wood.

Statements and Declarations

Competing Interests: The authors declare no competing financial or non-financial interests that are directly or indirectly related to the work submitted for publication.

Funding: The authors received no specific funding for this work.

Availability of data and materials The dataset analysed and the analysis code are available from the corresponding author upon reasonable request.

[Author contributions: JOA: Conceptualization, Data curation, Formal analysis, Investigation, Methodology, Writing–original draft, Supervision. **AAA:** Investigation, Writing–review and editing. **GKO:** Investigation, Writing–review and editing. **JKK**: Resources, Writing–review and editing. **EE**: Validation, Writing–Writing and editing. **FWO**: Supervision, Writing–review and editing.

References

Blakemore PA, Langrish TAG (2008) Effect of pre-drying schedule ramping on collapse recovery and internal checking with Victorian Ash eucalypts. Wood Science and Technology 42:473–492. https://doi.org/10.1007/s00226-008-0186-5

Brischke C, Welzbacher CR, Brandt K, Rapp AO (2007) Quality control of thermally modified timber: Interrelationship between heat treatment intensities and CIE L*a*b* color data on homogenized wood samples. Holzforschung 61(1):19–22. https://doi.org/10.1515/HF.2007.004

Bytner O, Drożdżek M, Laskowska A, Zawadzki J (2022) Temperature, time, and interactions between them in relation to colour parameters of black poplar (*Populus nigra* L.) Thermally modified in nitrogen atmosphere. Materials 15:824. https://doi.org/10.3390/ma15030824

Candelier K, Thévenon M-F, Pétrissans A, et al (2016) Control of wood thermal treatment and its effects on decay resistance: A review. Annals of Forest Science 73:571–583. https://doi.org/10.1007/s13595-016-0541-x

Esteves B, Pereira H (2008) Wood modification by heat treatment: A review. BioResources 4:370–404. https://doi.org/10.15376/biores.4.1.370-404

González-Peña MM, Hale MDC (2009) Colour in thermally modified wood of beech, Norway spruce and Scots pine. Part 1: Colour evolution and colour changes. Holzforschung 63:385–393. https://doi.org/10.1515/HF.2009.077

Hill CAS (2006) Wood modification: Chemical, thermal and other processes. John Wiley & Sons, Chichester

Kauman WG (1964) Cell collapse in wood. Holz als Roh- und Werkstoff 22:183–196

Navi P, Sandberg D (2009) Thermo-Hydro-Mechanical Wood Processing. EPEL Press, Boca Raton.

Nishino Y, Janin G, Chanson B, Détienne P, Gril J, Thibaut B (1998) Colorimetry of wood specimens from French Guiana. J Wood Sci 44:3–8.

Matsuo M, Yokoyama M, Umemura K, et al (2011) Color changes in wood during heating: Kinetic analysis by applying a time–temperature superposition method. Applied Physics A 99:47–52. https://doi.org/10.1007/s00339-010-5542-2

Metsä-Kortelainen S, Antikainen T, Viitaniemi P (2006) The water absorption of sapwood and heartwood of Scots pine and Norway spruce heat-treated at 170 °c, 190 °c, 210 °c and 230 °c. Holz als Roh- und Werkstoff 64:192–197. https://doi.org/10.1007/s00107-005-0063-y

Owusu FW (2008) *Turraeanthus africanus* (Welw. Ex C.DC.) Pellegr. In: Louppe D, Oteng-Amoako AA, Brink M (eds) PROTA (plant resources of tropical africa). PROTA, Wageningen, Netherlands

Quartey GA, Marfo ED, Wereko EY, Godwyll K-B (2025) The thermo-chemical modification of Avodire (*turraeanthus africanus*) to enhance its performance for interior applications. Materials Sciences and Applications 16:367–375. https://doi.org/10.4236/msa.2025.167021

Repellin V, Guyonnet R (2005) Evaluation of heat-treated wood swelling by differential scanning calorimetry in relation to chemical composition. Holzforschung 59:28–34. https://doi.org/10.1515/HF.2005.005

Sandberg D, Kutnar A, Karlsson O, Jones D (2021) Wood modification technologies: Principles, sustainability, and the need for innovation. CRC Press, Boca Raton, FL

Tjeerdsma BF, Militz H (2005) Chemical changes in hydrothermal treated wood: FTIR analysis of combined hydrothermal and dry heat-treated wood. European Journal of Wood and Wood Products (Holz als Roh- und Werkstoff) 63:102–111. https://doi.org/10.1007/s00107-004-0532-8

513 **Table 1** Experimental design and response definitions.

Element	Definition	Role in inference
Groups	Control (105 °C, 24 h); 160, 180, 200, 220 °C for 3 h in dry air; $n = 10$ each	Contrasts against the drying control
Optical	ΔL^*, Δa^*, Δb^*, ΔE^*_{ab} (Eq. 1), $\Delta E^*_{ab,\mathrm{dc}}$ (Eq. 2)	Optical family
Gravimetric	AWL from the post-treatment mass (Eq. 3)	Gravimetric family
Hygroscopic	MC_{336}; M_∞, τ, β (Eq. 5); MEE	Capacity, timescale, shape
Structural	Radial, tangential, longitudinal shrinkage; volume retention; oven-dry density; ϕ_{est} (Eq. 4); swelling	Structural family
Unit of analysis	Specimen within one supply lot	Within-lot inference only

514

515

Table 2 Treatment effects relative to the 105 °C drying control: difference in group means with Welch 95 % confidence interval ($n = 10$ per group). * Permutation $p < 0.05$ after Holm adjustment within the response family (optical, gravimetric, hygroscopic, structural). Hedges g for every contrast is plotted in Fig. 1a. Radial and tangential refer to the specimen thickness and width of flat-sawn stock.

Response	160 °C	180 °C	200 °C	220 °C
ΔL^*	-0.41 $[-2.50, 1.68]$	-3.72^* $[-6.30, -1.14]$	-16.40^* $[-20.80, -11.99]$	-30.97^* $[-33.43, -28.52]$
Δa^*	1.37^* $[0.95, 1.79]$	2.86^* $[2.51, 3.21]$	5.78^* $[5.27, 6.30]$	8.11^* $[7.71, 8.51]$
Δb^*	3.36^* $[2.43, 4.28]$	5.29^* $[4.61, 5.98]$	5.55^* $[3.95, 7.15]$	1.50 $[-0.07, 3.07]$
ΔE^*_{ab}	3.42^* $[1.89, 4.95]$	7.09^* $[5.29, 8.89]$	18.12^* $[14.62, 21.62]$	31.13^* $[28.88, 33.37]$
AWL (%)	0.31^* $[0.00, 0.62]$	1.04^* $[0.74, 1.33]$	1.78^* $[1.36, 2.20]$	2.85^* $[2.50, 3.20]$
MC_{336} (%)	-0.37^* $[-0.58, -0.17]$	-0.67^* $[-0.92, -0.41]$	-1.79^* $[-2.05, -1.54]$	-3.33^* $[-3.59, -3.06]$
M_∞ (%)	-0.30 $[-0.59, -0.02]$	-0.48^* $[-0.77, -0.19]$	-1.49^* $[-1.75, -1.24]$	-3.25^* $[-3.53, -2.96]$
τ (h)	3.3 $[-4.6, 11.1]$	14.8^* $[7.1, 22.5]$	27.4^* $[19.8, 35.1]$	20.4^* $[13.4, 27.3]$
Radial shrinkage (%)	-0.29 $[-0.79, 0.21]$	5.82^* $[5.43, 6.20]$	0.24 $[-0.31, 0.79]$	0.39 $[-0.06, 0.83]$
Tangential shrinkage (%)	0.11 $[-0.38, 0.59]$	1.35 $[0.39, 2.30]$	-0.12 $[-0.54, 0.31]$	0.32 $[-0.10, 0.74]$
Volume retention (%)	0.12 $[-0.30, 0.55]$	-7.74^* $[-8.55, -6.93]$	-0.17 $[-0.64, 0.30]$	-0.76 $[-1.20, -0.31]$
Oven-dry density (g cm^{-3})	0.004 $[-0.024, 0.031]$	0.068^* $[0.041, 0.096]$	0.000 $[-0.024, 0.023]$	-0.002 $[-0.025, 0.021]$
Estimated porosity	-0.003 $[-0.021, 0.016]$	-0.046^* $[-0.064, -0.027]$	0.000 $[-0.015, 0.016]$	0.001 $[-0.014, 0.017]$
Swelling (%)	-0.28 $[-0.83, 0.26]$	9.11^* $[8.10, 10.12]$	-0.46 $[-1.02, 0.10]$	-1.18^* $[-1.73, -0.64]$

Table 3 Cross-domain response summary. Onset: lowest temperature differing from the control (Holm-adjusted permutation test). Level: O, observation; S, supported interpretation; U, unresolved mechanism.

Response	Onset (°C)	Behaviour	Interpretation (level)
Redness (Δa^*)	160	Monotonic rise	Early optical pathway (S); chemistry (U)
Lightness (ΔL^*)	180	Small, then steep fall above 180 °C	Higher-threshold darkening (S)
Yellowness (Δb^*)	160	Rise to 200 °C, reversal at 220 °C	Accumulation then masking (U)
ΔE^*_{ab}	160	Composite of the three	Not one reaction coordinate (S)
AWL	160 (test-dependent)	Small, near-linear rise to 2.85 %	Low-level values may include moisture (U)
MC_{336} and M_∞	160 and 180	Large fall at 200–220 °C	Fewer accessible sites (S); composition (U)
τ	180	Peak at 200 °C	Slower approach to terminal state (O)
β	none	≈ 0.72; possible small decline	Shape approximately invariant (S)
Structure	180 only	Non-monotonic anomaly	Collapse-like densification or design effect (U)

List of Figures

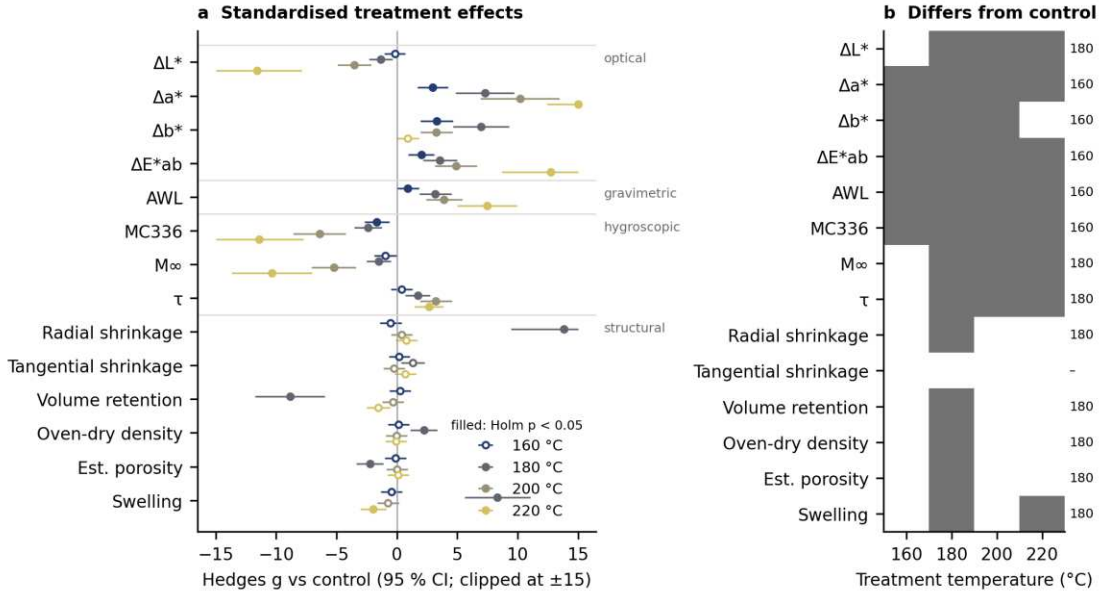


Fig. 1 Cross-domain response map. (a) Hedges g (95 % CI) of each treated group against the 105 °C drying control; filled symbols, Holm-adjusted permutation $p < 0.05$ within the response family. (b) Temperatures at which each response differs from the control; the right-hand column gives the onset.

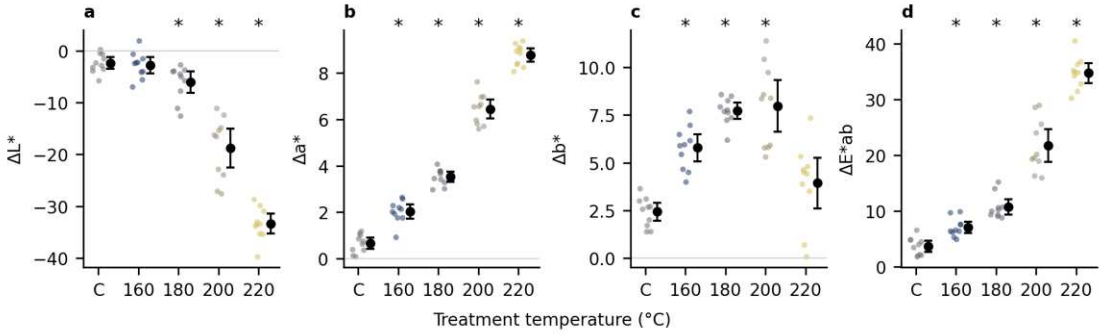
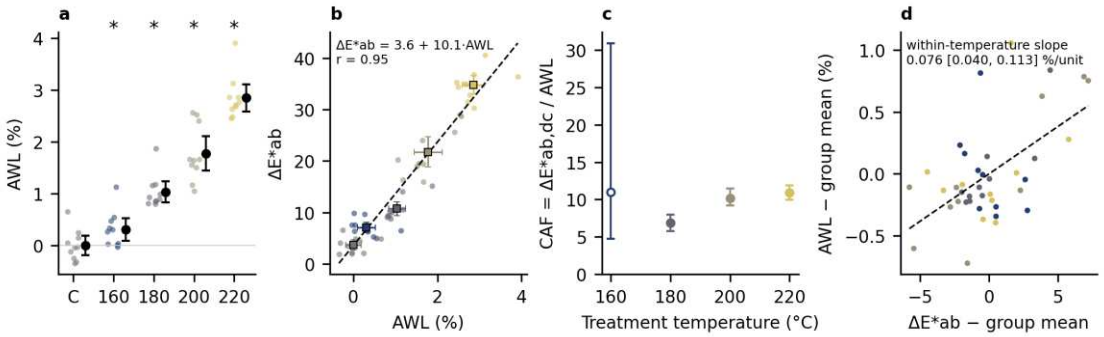
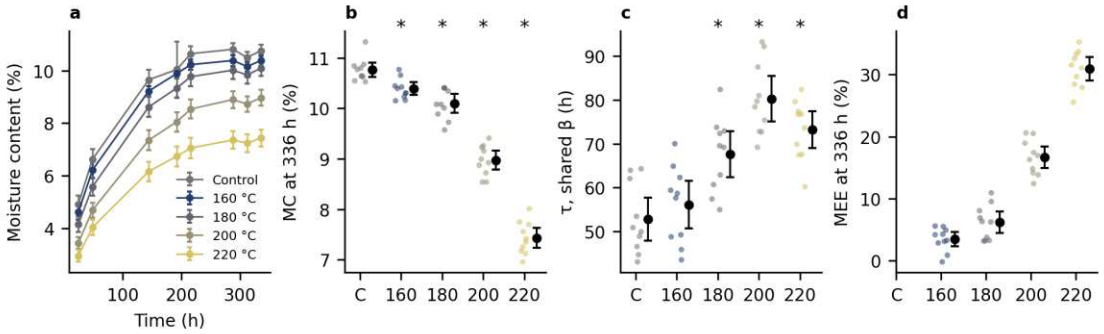


Fig. 2 Decomposition of the optical response: (a) ΔL^*, (b) Δa^*, (c) Δb^*, (d) ΔE^*_{ab}. Points, specimens; black symbols, group mean with 95 % CI; asterisks, Holm-adjusted difference from the control (C).



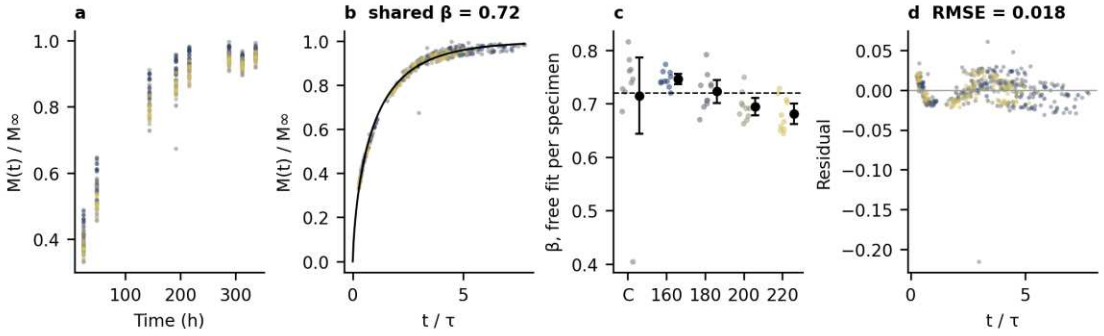
535

536 **Fig. 3** Colour versus mass loss. (a) AWL by group. (b) ΔE^*_{ab} against AWL for all specimens, with group centroids
537 ($\pm$95 % CI) and the pooled fit. (c) Colour-amplification factor with bootstrap 95 % interval; open symbol, not
538 interpreted. (d) Within-temperature relationship: deviations of AWL and ΔE^*_{ab} from their group means for treated
539 specimens.



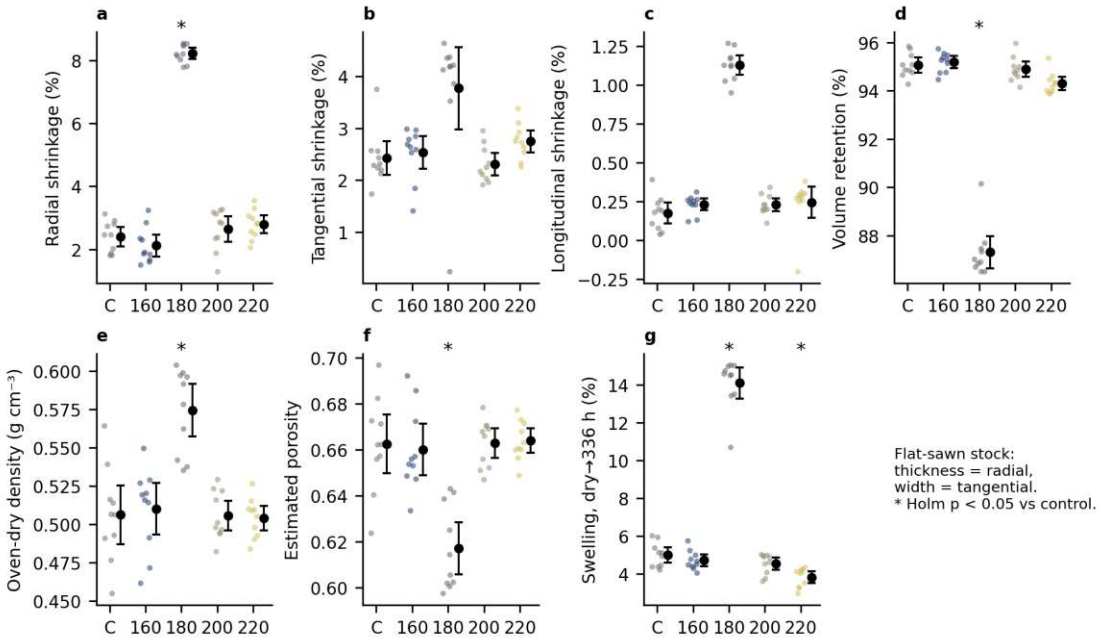
540

541 **Fig. 4** Moisture uptake in ambient air. (a) Group-mean uptake curves ($\pm$SD). (b) 14-day terminal moisture content
542 MC_{336}. (c) Characteristic time τ under the shared β. (d) MEE at 336 h.



543

544 **Fig. 5** Sorption master curve. (a) Normalised uptake $M(t)/M_\infty$ against time. (b) The same data against t/τ with the
545 shared-β Weibull curve. (c) β from free fits per specimen; dashed line, shared β. The low control value is TA-C-6.
546 (d) Residuals about the master curve by group.



547

548 **Fig. 6** Structural response: (a) radial (thickness), (b) tangential (width) and (c) longitudinal shrinkage; (d) volume
549 retention; (e) oven-dry density; (f) estimated porosity; (g) swelling over the 14-day uptake. Labelled “180 °C
550 structural anomaly” in the text; its cellular basis was not imaged.

551

Supplementary material

Table S1 Group means ± SD ($n = 10$). The control was oven-dried at 105 °C for 24 h. M_∞ and τ are from the shared-β Weibull fit.

Property	Control	160 °C	180 °C	200 °C	220 °C
L^* before	80.5 ± 2.6	79.5 ± 2.9	80.6 ± 2.0	81.1 ± 2.6	79.9 ± 2.3
L^* after	78.2 ± 2.3	76.7 ± 2.6	74.5 ± 2.1	62.4 ± 4.0	46.5 ± 2.7
a^* after	2.91 ± 0.37	4.32 ± 0.38	5.60 ± 0.39	8.69 ± 0.74	10.87 ± 0.42
b^* after	23.05 ± 2.14	26.02 ± 1.28	28.52 ± 1.42	28.92 ± 0.68	24.20 ± 0.80
C^*_{ab} after	23.24 ± 2.12	26.38 ± 1.28	29.07 ± 1.46	30.20 ± 0.82	26.54 ± 0.68
h_{ab} after (°)	82.8 ± 1.1	80.6 ± 0.8	78.9 ± 0.3	73.3 ± 1.1	65.8 ± 1.2
ΔL^*	-2.36 ± 1.84	-2.77 ± 2.53	-6.08 ± 3.33	-18.76 ± 6.03	-33.33 ± 3.13
Δa^*	0.66 ± 0.39	2.03 ± 0.49	3.52 ± 0.36	6.44 ± 0.66	8.77 ± 0.46
Δb^*	2.43 ± 0.76	5.78 ± 1.15	7.72 ± 0.69	7.98 ± 2.17	3.93 ± 2.13
ΔC^*_{ab}	2.49 ± 0.74	6.01 ± 1.18	8.16 ± 0.68	9.14 ± 2.06	6.15 ± 2.00
ΔH^*_{ab}	0.46 ± 0.30	1.20 ± 0.41	2.32 ± 0.42	4.67 ± 0.84	7.39 ± 0.80
ΔE^*_{ab}	3.65 ± 1.60	7.07 ± 1.65	10.74 ± 2.17	21.77 ± 4.77	34.77 ± 2.90
$\Delta E^*_{ab,\mathrm{dc}}$	0.00 ± 1.60	3.42 ± 1.65	7.09 ± 2.17	18.12 ± 4.77	31.13 ± 2.90
AWL (%)	0.00 ± 0.30	0.31 ± 0.35	1.04 ± 0.32	1.78 ± 0.54	2.85 ± 0.42
MC_{336} (%)	10.76 ± 0.23	10.39 ± 0.20	10.10 ± 0.30	8.97 ± 0.30	7.43 ± 0.32
MEE (%)	0.0 ± 2.1	3.5 ± 1.9	6.2 ± 2.8	16.6 ± 2.8	30.9 ± 3.0
M_∞ (%)	11.06 ± 0.27	10.75 ± 0.32	10.57 ± 0.34	9.56 ± 0.27	7.81 ± 0.32
τ (h)	52.9 ± 7.9	56.1 ± 8.8	67.7 ± 8.5	80.3 ± 8.3	73.2 ± 6.8
Radial shrinkage (%)	2.41 ± 0.49	2.12 ± 0.57	8.22 ± 0.28	2.64 ± 0.66	2.79 ± 0.46
Tangential shrinkage (%)	2.43 ± 0.53	2.53 ± 0.51	3.77 ± 1.28	2.31 ± 0.35	2.75 ± 0.34
Longitudinal shrinkage (%)	0.18 ± 0.11	0.23 ± 0.06	1.13 ± 0.10	0.23 ± 0.07	0.24 ± 0.16
Volume retention (%)	95.1 ± 0.5	95.2 ± 0.4	87.3 ± 1.1	94.9 ± 0.5	94.3 ± 0.4
Density as received (g cm^{-3})	0.534 ± 0.031	0.540 ± 0.029	0.562 ± 0.027	0.542 ± 0.014	0.543 ± 0.012
Oven-dry density (g cm^{-3})	0.506 ± 0.031	0.510 ± 0.027	0.574 ± 0.028	0.506 ± 0.016	0.504 ± 0.013
Estimated porosity	0.663 ± 0.021	0.660 ± 0.018	0.617 ± 0.018	0.663 ± 0.010	0.664 ± 0.009
Swelling (%)	4.99 ± 0.65	4.71 ± 0.50	14.10 ± 1.33	4.53 ± 0.53	3.81 ± 0.50

Table S2 Moisture-uptake shape. $M(t) = M_\infty[1 - \exp(-(t/\tau)^\beta)]$ fitted to all 50 curves (400 observations) with specimen-specific M_∞ and τ and four treatments of β. ΔAICc is relative to the best model; the right-hand columns omit specimen TA-C-6, whose 192 h reading lies below its 144 h reading. Group β (profile estimate, 95 % specimen-bootstrap interval): all: 0.720 [0.700, 0.730] ; C: 0.720 [0.655, 0.765] ; 160 °C: 0.745 [0.740, 0.755] ;

180 °C: 0.725 [0.705, 0.745] ; 200 °C: 0.695 [0.680, 0.710] ; 220 °C: 0.685 [0.665, 0.700]. Master-curve RMSE: 0.018 (all), 0.014 (without TA-C-6).

		All 50 curves		Without TA-C-6	
β model	Parameters	RSS	ΔAICc	RSS	ΔAICc
first-order (beta = 1)	100	46.99	474.0	38.67	617.1
shared beta	101	14.24	0.0	7.94	0.0
beta per group	105	14.03	8.6	7.65	0.1
beta per specimen	150	12.68	164.4	7.28	172.3

Table S3 Anhydrous weight loss on two moisture bases, mean ± SD ($n = 10$). Upper: post-treatment mass with MC_0 from the controls' first 105 °C weighing (10.91 %; Eq. 3). Lower: second 105 °C oven-dry mass with MC_0 from the controls' second drying (11.11 %), so both masses refer to the 105 °C state. Gap: water removed by treatment that the 105 °C state retains. Re-drying change: second oven-dry mass relative to post-treatment mass.

Group	AWL, upper (%)	AWL, lower (%)	Gap (pp)	Re-drying change (%)
Control	0.00 ± 0.30	0.00 ± 0.31	0.00 ± 0.05	-0.18 ± 0.05
160 °C	0.31 ± 0.35	-0.03 ± 0.35	0.34 ± 0.03	0.16 ± 0.03
180 °C	1.04 ± 0.32	0.35 ± 0.34	0.68 ± 0.03	0.51 ± 0.03
200 °C	1.78 ± 0.54	1.32 ± 0.55	0.46 ± 0.03	0.29 ± 0.03
220 °C	2.85 ± 0.42	2.45 ± 0.40	0.40 ± 0.05	0.24 ± 0.05

Table S4 Moisture-uptake timescales by group, median [IQR]. τ from the shared-β fit ($\beta = 0.72$, Table S1); $t_{50} = \tau(\ln 2)^{1/\beta}$ and $t_{90} = \tau(\ln 10)^{1/\beta}$; 0 of 50 specimens had t_{90} beyond the last weighing (336 h). RMSE: per-specimen free-β fit, percentage points of moisture content, 8 weighings; 0 of 50 free fits reached a parameter bound (M_∞ 0–40 %, τ 1–5000 h, β 0.2–2.0).

Group	n	τ (h)	t_{50} (h)	t_{90} (h)	RMSE
Control	10	50.5 [47.2, 60.0]	30.3 [28.4, 36.1]	161 [150, 191]	0.158 [0.151, 0.174]
160 °C	10	58.2 [49.0, 61.6]	35.0 [29.4, 37.0]	185 [156, 196]	0.145 [0.139, 0.155]
180 °C	10	69.5 [61.3, 72.9]	41.8 [36.9, 43.8]	221 [195, 232]	0.149 [0.144, 0.151]
200 °C	10	79.1 [73.5, 85.9]	47.6 [44.2, 51.7]	252 [234, 274]	0.130 [0.123, 0.137]
220 °C	10	75.2 [68.3, 77.3]	45.2 [41.0, 46.5]	240 [217, 246]	0.088 [0.084, 0.099]

Apparent temperature sensitivity. Group-mean changes at the single 3 h hold were regressed as $\ln|\Delta Y| = \ln A - E_{a,\mathrm{app}}/(RT)$ over the four treatment temperatures. The slopes are compact descriptors of temperature sensitivity, not activation energies: ΔL^* 76.4 kJ mol^{-1} ($R^2 = 0.99$), ΔH^*_{ab} 54.7 (1.00), ΔE^*_{ab} 48.6 (0.99), Δa^* 44.4 (0.99) and AWL 64.3 (0.96). Δb^* and ΔC^*_{ab} were non-monotonic and no slope was assigned.

Earlier AWL definition. The 2026-09 draft computed AWL from the second 105 °C oven-dry mass with a baseline from the first, which gave 0.15, 0.53, 1.50 and 2.62 % and a control value of 0.18 %. The reconciliation is documented in the repository (`paper/reconciliation.md`).